Direct Immobilization of Phosphine-Rhodium Complex on MCM-41 for Propene Hydroformylation*

CAI Yang, LI Zhi-hua, YANG Yi-quan and YUAN You-zhu**

State Key Laboratory for Physical Chemistry of Solid Surfaces, Department of Chemistry, Xiamen University, Xiamen 361005, P. R. China

Received July 2, 2001

MCM-41 molecular sieve supported Rh-PPh_3 catalysts were prepared by the *in-situ* assembling of the metal complex from smaller moieties of $Rh(acac)(CO)_2$ and ligand of PPh_3. The resulted guest/host materials(Rh-PPh_3/MCM-41) were characterized by X-ray powder diffraction, FTIR and $^{31}P(^1H)$ NMR, and served as catalysts for propene hydroformylation. The results showed negligible change in MCM-41 framework after propene hydroformylation at 393 K. Higher hydroformylation activities were obtained on Rh-PPh_3/MCM-41 catalysts compared to that on Rh-PPh_3/SiO_2.

Keywords MCM-41 mesoporous molecular sieve, Hydroformylation, Propene, Rh-phopshine complex

Article ID 1005-9040(2002)-03-311-05

Introduction

Heterogenization of $HRh(CO)(PPh_3)_3$(PPh_3: triphenylphosphine) for hydroformylation and selective hydrogenation has received considerable attention in the past several decades from both academic and industrial interests[1]. Besides the milestone preparation of water-soluble TPPTS and the corresponding rhodium-phosphine complexes such as $HRh(CO)(TPPTS)_3$ (**1**)[2,3], supported liquid-phase catalysts (SLPC)[4—6] and supported aqueous-phase catalysts (SAPC)[7] are known as attractive alternatives of heterogenized catalysts for olefin hydroformylation.

Studies on zeolite-encapsulated rhodium species as hydrofoymylation catalysts have been well documented[8—12]. The major drawback for the use of conventional zeolites is the small pore size, which makes it difficult for substrates to diffuse and approach to the active sites and for products to diffuse out of the pores when the ligands with large molecule sizes are employed[13]. Some examples of reported mesoporous solids, including silica, alumina and pillared smectite clay are invariably amorphous or *para*-crystalline, and their pores are irregularly spaced and broadly distributed in size[4—6,14]. The search for new and larger-pore zeolites will be very helpful in creating catalysts. Of particular interest is a multi-dimensional, extra-large pore material. The development of the mesoporous material, named MCM-41, provided a new possible candidate as a solid support for immobilization of homogeneous catalysts. MCM-41 has been produced and is characterized by pore diameters that can be adjusted between 1.8 and 20 nm. Its large pore size allows the passage of large molecules such as organic reactants and metal complexes through the pores to reach the surface of the channel. In addition, the regular pore size of MCM-41 can provide shape selectivity that is not provided by silica gel. It possesses regular arrays of uniform channels, higher surface area and exceptionally high sorption capacities of cyclohexane and benzene[15]. Special properties in the emission spectroscopy and positive effects in the hydrodesulfurization catalysis of thiophene have been observed by using MCM-41 as the carrier for encapsulating ruthenium complexes[16] and metal oxides such as Ni- and Mo-oxides[17], respectively.

SiO_2 and Al_2O_3 immobilized $HRh(CO)(PPh_3)\cdot PPh_3$ catalysts yielded an excellent SLPC system for propene hydroformylation under mild reaction conditions[4—6]. The immobilization of $Rh(PPh_3)_3Cl$ on phosphonated MCM-41 resulted in a stable hydrogenation catalyst with turnover frequency three times higher than that of $Rh(PPh_3)_3Cl$ in the hydrogenation of cyclohexene[18]. We used MCM-41 mesoporous molecular sieve with $Rh(acac)(CO)_2$ and PPh_3

* Supported by the National Natural Science Foundation of China(Nos. 29873037, 20023001 and 20021002), State Key Project for Fundamental Research(No. G200004808) and the Ministry of Education of China.

** To whom correspondence should be addressed.

moeties directly supported as propene hydroformylation catalyst. The MCM-41 materials used are characterized by pore diameters of 2—4 nm. The samples thus prepared were characterized by various spectroscopic methods before and after propene hydroformylation, such as XRD, FTIR, BET, and NMR.

Experimental

1 Synthesis of MCM-41-type Molecular Sieves

Si-MCM-4 and Al-MCM-41 were obtained under typical hydrothermal conditions[19,20] by using tetraethylorthosilicate(TEOS) as the silica source. MCM-41 materials with different pore sizes were attained by using surfactants with different chain lengths. Aluminosilicate MCM-41 was synthesized by the addition of $Al_2(SO_4)_3$ as aluminium source to the synthesis mixture. The surface area, pore volume and pore diameters of pure MCM-41 and Al-modified MCM-41 materials are listed in Table 1.

Table 1 Effect of surfactant chain length and n(Si)/n(Al) ratio on MCM-41 BET surface area, pore volume and pore diameter

Supporter	n^*	n_{Si}/n_{Al}	S_{BET}/($m^2 \cdot g^{-1}$)	Pore volume/($cm^3 \cdot g^{-1}$)	Pore diameters/nm
Si-MCM-41-A	16	∞	1 003	0.96	2.8—3.2
Si-MCM-41-B	14	∞	1 062	0.68	2.0—2.4
Si-MCM-41-C	12	∞	1 193	0.66	1.6—2.0
Al-MCM-41-A	16	100	845	0.84	2.8—3.2
Al-MCM-41-B	16	80	848	0.88	2.8—3.2
Al-MCM-41-C	16	60	848	0.89	2.8—3.6
Al-MCM-41-D	16	40	565	0.72	2.8—3.6
SiO_2			380	1.03	6—12
NaY			985	0.35	~0.9
NaZSM-5		38	376	0.13	~0.7

* n is the surfactant chain length of $C_nH_{2n+1}(CH_3)_3N^+$.

2 Synthesis of Catalysts

$Rh(acac)(CO)_2$ was prepared by means of the known method, its IR adsorption peaks agreed with those in the literature[21]: 2 066(s), 1 599 (s), 1 526(s), 1 382(s), 1 350(s) and 763(w) cm^{-1}.

MCM-41 and other supports were pressed and crashed to 80—100 meshes before impregnation of rhodium and phosphine moieties. The supported Rh-phosphine catalysts were prepared by an incipient wetness technique. A dichloromethane solution of $Rh(acac)(CO)_2$(0.05 mmol/mL) was poured into a Schlenk flask containing 1.0 g degassed MCM-41. After the mixture was further degassed by vacuum boiling, argon was introduced and the slurry was kept at room temperature for 1 h while the vibration was carried out. The dichloromethane was removed under vacuum at room temperature. Incipient wetness was then used to add a dichloromethane-solution of PPh_3 to the above sample. The final product was a dry, free-flowing-yellow powder and noted as Rh-PPh_3/MCM-41.

3 Characterization

The XRD patterns were recorded on a Rigaku D/Max-C X-ray powder diffractometer with Cu $K\alpha$ radiation. The scanning range was 1.6°—30° with a step size of 0.01° at a scanning rate of 2°/min. There are no XRD reflexes in the usual range above 10°.

The solution $^{31}P\{^1H\}$ NMR spectra were recorded on a Varian FT Unity+ 500 spectrometer at 200 MHz and room temperature. ^{31}P NMR chemical shifts were reported relative to 85% H_3PO_4. The samples in the NMR tube were introduced about 40% benzene before the measurements. The FTIR spectra were measured on a Nicolet-740 spectrometer with a resolution of 4 cm^{-1}. The surface areas of the samples were measured at 77 K by means of a conventional BET nitrogen adsorption method and a SORPTOMATIC-1900 machine.

4 Catalytic Reaction

The propene hydroformylation reaction was performed in a high-pressure fixed-bed flow reactor connecting an on-line gas chromatgraph equipped with an FID detector and a column of Porapak Q. The V(Propene)/V(CO)/V(H_2) ratio used here was always 1∶1∶1. The results showed that the total hydrogenation products were lower than 1.0% under the present experiment conditions. All the data were taken at 2 h after the start of the reaction, unless otherwise noted.

Results and Discussion

1 Catalytic Performance

Fig. 1 shows the conversion of propene and the molar ratio of normal-to *iso*-butyl aldehyde(n/i) as the function of time-on-stream for a series of MCM-41 and SiO_2-supported Rh-PPh_3 catalysts. The conversion and the selectivity of these catalysts were time-independent after the reaction for 100 min. The coverage with PPh_3 is defined as[5]:

$$\theta_{PPh_3} = \frac{[c(PPh_3)\, N_{Av} S(PPh_3)]}{S_{BET}} \quad (1)$$

where $c(PPh_3)$ is the loading amount of PPh_3 on the support (mol g-support^{-1}), S(PPh$_3$) is the cross-sectional area of a PPh$_3$ molecule(1.2×10^{-18} m^2), N_{Av} is Avogadro's number (6.02×10^{23} molecules/mol), and S_{BET} is the BET surface area of the support (Table 1). Table 1 shows that the MCM-41 materials prepared with CTAB as the template have an average pore diameter of about 3.0 nm. The average pore diameter increased slightly with the increase of the alkyl chain length of the template, but there was no significant change in pore size with Si/Al molar ratio. The high surface area in the range of 560—1 200 m^2/g and the pore volume greater than 0.5 cm^3/g for all the samples are indicative of the formation of the mesoporous structure.

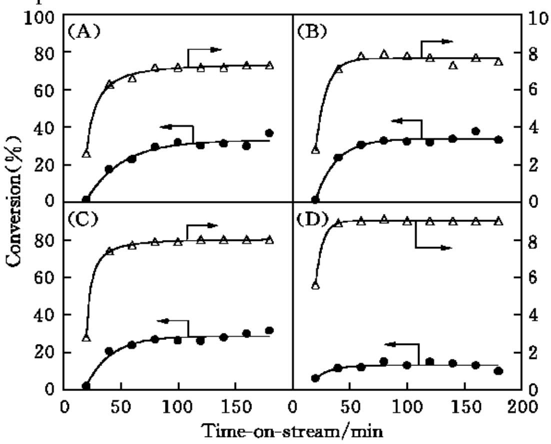

Fig. 1 The propene hydroformylation performance as a function of time-on-stream on Rh-PPh$_3$/MCM-41 and Rh-PPh$_3$/SiO$_2$ catalysts

Reaction conditions: 393 K, 1.0 MPa, $V(C_3H_6)/V(CO)/V(H_2)$ = 1/1/1, GHSV = 9 000 mL (STP) h^{-1} (g · catal.)$^{-1}$; 0.05 mmol Rh(acac)(CO)$_2$ were loaded on 1.0 g support with the corresponding P/Rh molar ratio at 9; data taken after 2 h of reaction operation.
(A) Rh-PPh$_3$/Si-MCM-41-A; (B) Rh-PPh$_3$/Si-MCM-41-B; (C) Rh-PPh$_3$/Al-MCM-41-B; (D) Rh-PPh$_3$/SiO$_2$.

It is found from Table 2 that the catalytic activity of lower coverage catalysts, per unit weight of rhodium, is appreciably higher than that of the catalysts with a higher coverage. As a common feature, much higher activity but lower n/i molar ratio on Rh-PPh$_3$/MCM-41 catalysts than that on Rh-PPh$_3$/SiO$_2$ has been obtained. We estimated taht this result was mainly due to the contribution made by the surface area of the supports. The minor difference in catalytic activity and n/i molar ratio among the MCM-41 supporters prepared from surfactants with different chain length and n(Si)/n(Al) is probably due to the small sizes of reactants and products.

Table 2 The results of propene hydroformylation on Rh-PPh$_3$/MCM-41 and Rh-PPh$_3$/SiO$_2$ catalysts*

Support	θ_{PPh_3}	Conv. of C_3H_6(%)	TOF/ s^{-1}	STY/ (mol · h^{-1} · g$_{Rh}^{-1}$)	n/i
Si-MCM-41-A	0.324	31.6	0.24	8.23	7.5
Si-MCM-41-B	0.306	33.6	0.25	8.75	7.5
Si-MCM-41-C	0.272	25.4	0.19	6.61	7.8
Al-MCM-41-A	0.385	26.1	0.19	6.79	7.3
Al-MCM-41-B	0.383	28.1	0.21	7.31	8.0
Al-MCM-41-C	0.383	35.2	0.26	9.16	7.5
Al-MCM-41-D	0.575	30.8	0.23	8.02	7.6
SiO$_2$	0.855	13.6	0.10	3.54	9.0

* All the reaction conditions were the same as those in Fig. 1.

Table 3 shows the activities of the Rh-catalysts with different Rh-loading in Rh-PPh$_3$/MCM-41 and Rh-PPh$_3$/SiO$_2$. The conversion increased accordingly, as expected, but the selectivity to butyl aldehyde increased with the Rh-loading weight, which was probably due to the concentration effect at some locations or/and the blocking effect of pore channel while a high surface area was kept after immobilization of the Rh-PPh$_3$ species. This was not the case for using NaY, NaZSM-5 and SiO$_2$ as supports. The results again demonstrate that MCM-41 supported catalyst showed a superior catalytic activity in the case of coverage studied. The MCM-41 supported Rh-PPh$_3$ catalysts with a PPh$_3$/Rh molar ratio of 9 and a coverage degree θ higher than 0.3 were found not to be evidently deactivated after the reaction for 8 h at 393 K, while the ones with coverage degree lower than 0.3 presented a significant deactivation after the reaction for 4 h.

Table 3 Propene hydroformylation on Rh-PPh$_3$/MCM-41 and Rh-PPh$_3$/SiO$_2$ catalysts with different Rh-loading*

Support	Rh loading weight/ (mmol · g^{-1})	θ_{PPh_3}	Conv. of C_3H_6 (%)	TOF/ s^{-1}	STY/ (mol · h^{-1} · g$_{Rh}^{-1}$)	n/i
Si-MCM-41-A	0.025	0.162	18.1	0.27	9.42	6.5
	0.050	0.324	31.6	0.24	8.23	7.5
	0.075	0.486	32.3	0.16	5.61	7.8
	0.100	0.648	37.3	0.14	4.85	9.0
SiO$_2$	0.025	0.428	6.9	0.10	3.59	8.2
	0.050	0.855	13.3	0.10	3.46	9.0
	0.075	1.283	24.0	0.12	4.16	9.3
	0.100	1.711	32.3	0.12	4.20	9.4
NaY	0.100	0.660	13.9	0.05	1.81	11.0
NaZSM-5	0.100	1.729	16.1	0.06	2.10	10.7

* $n(P)/n(Rh)$ = 9. Reaction conditions are the same as in Fig. 1.

2 Characterization by BET, XRD, FTIR and NMR

Fig. 2 shows the N_2 adsorption-desorption isotherms of the representative as-synthesized MCM-41 and PPh_3-Rh/MCM-41 samples. It can be seen that the volume of N_2 adsorbed on the PPh_3-Rh/MCM-41 (at ~39.9 kPa) is higher (~500 mL/g) than that on as-synthesized samples (~400 mL/g). The t-plot analysis of the N_2-adsorption results revealed that a noticeable amount of mesopores was blocked due to the immobilization of PPh_3-Rh moieties.

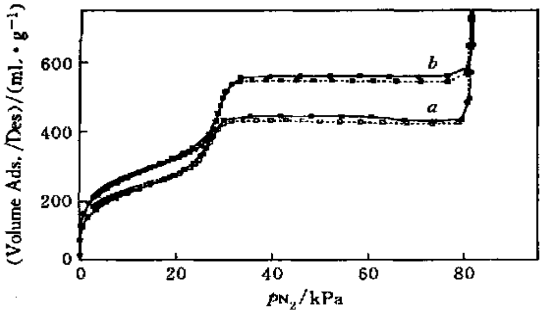

Fig. 2 N_2 adsorption-desorption isotherms at 77 K for the as-synthesized MCM-41 (*a*) and PPh_3-Rh/MCM-41 (*b*) samples

Fig. 3 shows the XRD patterns of the catalysts before and after propene hydroformylation. No X-ray diffraction lines of the Rh-PPh_3 complexes or the uncoordination crystalline PPh_3 were observed for the Rh-PPh_3/MCM-41 catalysts, suggesting a high dispersion of the Rh-$PPPh_3$ complexes and free PPh_3 species on the surfaces. The peaks for the samples after immobilization of Rh-Ph_3 and hydroformylation became broader and less intense, which indicated a lower degree of order and a lower regularity of the material. But a decrease in X-ray peak intensity is not necessarily an indication of a partial collapse of the structure or a lower regularity of the unidimensional pore arrangement.

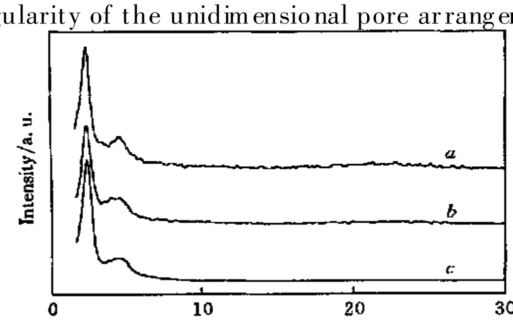

Fig. 3 XRD patterns for Si-MCM-41-A before and after immobilizing Rh-PPh_3

a. Si-MCM-41-A; *b*. as-prepared Rh-PPh_3/Si-MCM-41-A catalyst; *c*. Rh-PPh_3/Si-MCM-41-A catalyst after propene hydroformylation at 393 K for 3 h.

One explanation may be due to some organic material in the pore channel after immobilization and reaction, which disturbed the regular periodic variation of the electron density, resulting in the apparent decrease of hexagonal symmetry.

The IR spectra of pure MCM-41 and Al-MCM-41 are shown in Fig. 4(A). Among them there are no big differences. The three main peaks observed at about 1 085, 798 and 460 cm^{-1} could be assignable to the anti-symmetric and the symmetric stretching vibrations of Si—O—Si framework units, and to the deformation modes of the SiO_4 tetrahedra, respectively[22]. The peak at 960 cm^{-1} could be assigned to the Si—O stretching vibrations of Si—O—H. Fig. 4(B) shows the IR spectra of the catalysts before and after the propene hydroformylation. It is found that after hydroformylation two new bands at 2 039 and 1 922 cm^{-1} appeared [Fig. 4(B) *c*].

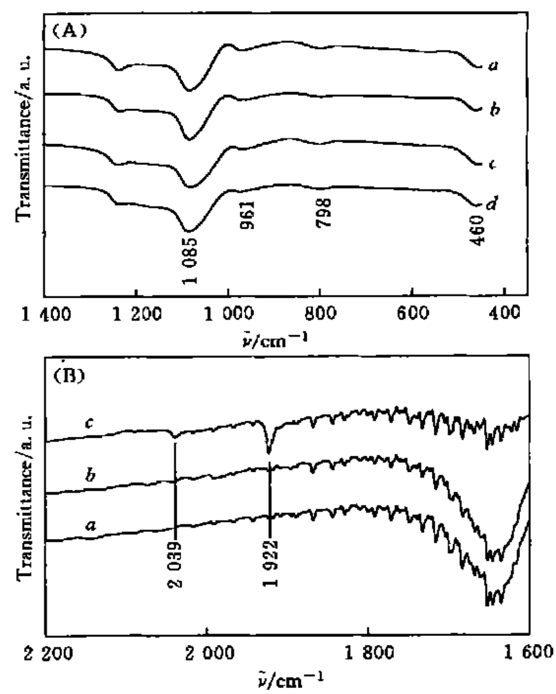

Fig. 4 FTIR spectra for MCM-41 with different Si/Al molar ratio (A) and Rh-PPh_3/MCM-41 before and after hydroformylation (B)

(A) *a*. Si-MCM-41-A; *b*. Al-MCM-41-A; *c*. Al-MCM-41-C; *d*. Al-MCM-41-D. (B) *a*. Si-MCM-41-A; *b*. Rh-PPh_3/Si-MCM-41-A; *c*. Rh-PPh_3/Si-MCM-41-A after propene hydroformylation at 393 K for 3 h.

By means of adding a proper amount of benzene to form a liquid-film on the catalyst surface, the chemical environments of phosphorous-containing species in the supported rhodium-phosphine complex catalyst or its precursor systems may be investigated by using the conventional solution $^{31}P(^{1}H)$ NMR spectroscopic method[23]. The results are shown in Fig. 5. The results of $^{31}P(^{1}H)$ NMR characterization show that a large part of phosphine ligand PPh_3 were not in the states of coordination in the catalysts prepared freshly by using Si-MCM-41 as the support and Rh(acac)$(CO)_2$ complex and PPh_3 as the precursors, and that a considerable quantity of the complexes containing phosphine ligand with a chemical shift with broadness at δ 41.7, besides the free phosphine species at δ −4.2, formed after hydroformylation for 3 h. On the other hand, the $^{31}P(^{1}H)$ NMR spectroscopy for Rh-PPh_3/Al-MCM-41 after the reaction for 3 h demonstrated that there existed several phosphorus peaks at δ 41.9, 33.4, and 28.8 with broadness. The results suggest that a coordination reaction between Rh^{I} species and PPh_3 occurred during the reaction.

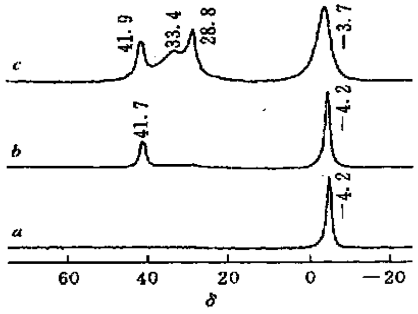

Fig. 5 $^{31}P(^{1}H)$ NMR spectra for Rh-PPh_3/Si-MCM-41-A(*a*), Rh-PPh_3/Si-MCM-41-A(*b*) after propene hydroformylation at 393 K for 3 h and Rh-PPh_3/Al-MCM-41-C (*c*) after propene hydroformylation at 393 K for 3 h

The chemical shifts for NMR phosphorus-31 peaks in Fig. 5 are likely due to the phosphorus species coordinated to Rh^{I} atoms. In addition, the IR bands at 2 039 and 1 922 cm^{-1} as shown in Fig. 4(B)*c* are assignable to a coordination unsaturated surface species of $[Rh(CO)_2(PPh_3)_2]$ as compared to the data reported in literature and are differed from those for $HRh(CO)(PPh_3)_x$ (x = 2, 3) and Rh(acac)(CO)(PPh_3)[24—27]. The species was possibly located in the pore channel of MCM-41 for the stabilization. It is reasonable to assume that there exists an interaction between the weak acidic MCM-41 surface and the basic ligand PPh_3, especially in the case of stronger acidic Al-MCM-41 used as the support, thus resulting in complicacy in the NMR observation (Fig. 5). The Rh-PPh_3 species formed on the catalyst surface was then readily transformed to the complex species $[HRh(CO)(PPh_3)_2]$ active for the propene hydroformylation under the reaction conditions[26, 27].

References

[1] Beller M., Cornils B., Frohning C. D., *et al*., *J. Mol. Catal. A*: *Chemical*, **1995**, *104*, 17
[2] Kuntz E. G., *US Patent*, 4 248 802, **1981**
[3] Kuntz E. G., *Chemtech*., **1987**, 570
[4] Gerritsen L. A., Van Meerkerk A., Vreugdenhil M. H., *et al*., *J. Mol. Catal*., **1980**, *9*, 139
[5] Hjortkjaer J., Scurrell M. S., Simonsen P., *et al*., *J. Mol. Catal*., **1981**, *12*, 179
[6] Pelt H. L., Gijsman P. J., Verburg R. P. J., *et al*., *J. Mol. Catal*., **1985**, *33*, 119
[7] Arhancet J. P., Davis M. E., Merola J. S. *et al*., *Nature*, **1989**, *339*, 454
[8] Rode E. J., Davis M. E., Hanson B. E., *J. Catal*., **1985**, *96*, 574
[9] Taylor D. F., Hanson B. E., Davis M. E., *Inorg. Chim. Acta*, **1987**, *128*, 55
[10] Davis M. E., Schnitzer J., Rossin J. A., *et al*., *J. Mol. Catal*., **1987**, *39*, 243
[11] Currie A. W. S., Andersen J. A. M., *Catal. Lett*., **1997**, *44*, 109
[12] Andersen J. A. M., Currie A. W. S., *Chem. Commun*., **1996**, 1 543
[13] Herron N., *J. Coord. Chem*., **1988**, *19*, 25
[14] Lenarda M., Ganzerla R., Storaro L., *et al*., *J. Mol. Catal*., **1992**, *72*, 75
[15] Kresge C. T., Leonowicz M. L., Roth W. J., *et al*., *Nature*, **1992**, *359*, 710
[16] Cao X. C., Wang Y., Li S. G., *et al*., *Chem. Res. Chinese Universities*, **2000**, *16*(1), 1
[17] Cui J., Yue Y. H., Sun Y., *et al*., *Chem. Res. Chinese Universities*, **1998**, *14*(3), 284
[18] Shyu S. G., Cheng S. W., Tzou D. L., *Chem. Commun*., **1999**, 2 337
[19] Ulagappan N., Rao C. N. R., *Chem. Commun*., **1997**, 1 047
[20] Becj J. S., Vartuli J. C., Roth W. J., *et al*., *J. Am. Chem. Soc*., **1992**, *114*, 10 834
[21] Bonati F., Wilkison G., *J. Chem. Soc*., **1964**, 3 156
[22] Roos K., Liepold A., Roschetilowski W., *et al*., *Stud. Surf. Sci. Catal*., **1994**, *84*, 389
[23] Arhancet J. P., Davis M. E., Merola J. S., *et al*., *J. Catal*., **1990**, *121*, 327
[24] Evans D., Yagupsky G., Wilkison G., *J. Chem. Soc. A*, **1968**, 2 660
[25] Yagupsky M., Brown C. K., Yagupsky G., *et al*., *J. Chem. Soc. A*, **1970**, 937
[26] Te M., Jiao F., Yin Y., *Chinese J. Mol. Catal*., **1992**, *6*, 193
[27] Zhang Y., Yuan Y., Chen Z., *et al*., *J. Xiamen Univ. (Natural Sci.)*, **1998**, *37*, 228